HHS Public Access

Author manuscript

Oncogene. Author manuscript; available in PMC 2015 March 23.

Published in final edited form as:

Oncogene. 2014 May 8; 33(19): 2495–2503. doi:10.1038/onc.2013.200.

miR-30 as a tumor suppressor connects EGF/Src signal to ERG and EMT

Chiao-Jung Kao[a], **Anthony Martiniez**[a], **Xu-Bao Shi**[b], **Joy Yang**[b], **Christopher P. Evans**[b], **Albert Dobi**[c], **Ralph W. deVere White**[b], and **Hsing-Jien Kung**[a,d,e,*]

[a]Department of Biochemistry and Molecular Medicine, University of California Davis, Davis, CA 95616, USA

[b]Department of Urology, University of California Davis, Sacramento, CA 95817, USA

[c]Center for Prostate Disease Research; Department of Surgery; Uniformed Services University of the Health Sciences; Rockville, MD 20852, USA

[d]National Health Research Institutes, Maioli County 35053, Taiwan

[e]Taipei Medical University, Taipei City 11031, Taiwan

Abstract

Src tyrosine kinase (Src) is implicated in the development of bone metastasis and castration-resistance of prostate cancer. Src inhibitors are currently being tested in clinical trials for such diseases. Understanding the molecular and cellular actions of Src inhibitors holds the key to future improvement of this line of therapy. Here we describe the microRNA (miRNA) expression profiles modulated by two Src inhibitors and demonstrate that the miR-30 family members are the most prominently induced species. Consistent with its tumor suppressor role, miR-30 is downmodulated by oncogenic signals such as epidermal growth factor (EGF) and hepatocyte growth factor (HGF), and is generally underexpressed in prostate cancer specimens. A number of epithelial to mesenchymal transition (EMT)-associated genes are predicted targets of miR-30. Among these genes the Ets Related Gene (ERG) is the most frequently overexpressed-oncogene in prostate cancer activated by genomic fusion events between promoter upstream sequences of the TMPRSS2 and coding sequences of ERG. We showed by ERG 3′UTR-reporter and mutagenesis assays that ERG is a direct target of miR-30. Overexpression of miR-30 in prostate cancer cells suppresses EMT phenotypes and inhibits cell migration and invasion. It also inhibits the *in vitro* and *in vivo* growth of VCaP cells, which depends on TMPRSS2-ERG for proliferation. TMPRSS2-ERG is generally regulated by androgen at the transcriptional level. Our finding reveals a new post-transcriptional mechanism of TMPRSS2-ERG regulation by Src and growth signals via miR-30 providing a rationale for targeting ERG positive castration resistant tumors with Src inhibitors.

[*]**Corresponding Author:** Hsing-Jien Kung Ph.D., Department of Biochemistry and Molecular Medicine, University of California, Davis, UCDMC Research 3, Room 2400, 4645 2nd Avenue, Sacramento, CA 95817, Ph: 916-734-1538, Fax: 916-734-2589, hkung@ucdavis.edu.

CONFLICT of INTEREST

The authors declare no conflicts of interest.

Supplementary Information accompanies the paper on the Oncogene website (http://www.nature.com/onc).

Keywords

Prostate cancer; EGF; Src; miRNA; ERG and EMT

INTRODUCTION

Src tyrosine kinase is widely expressed and implicated in the development of human malignancies including castration-resistance prostate cancer (1, 2). In mouse models, Src was found to synergize with the androgen receptor (AR) in the transformation of prostate epithelial cells to invasive adenocarcinoma (3). We showed previously that in prostate cancer cells, Src is complexed with focal adhesion kinase (FAK) and Etk tyrosine kinases, which trans-phosphorylate one another to induce migration and invasion (4). Src also regulates osteoclastic activity and promotes bone metastasis of prostate cancer cells (5, 6). Regarding its role in castration-resistant prostate cancer, Src is shown to activate AR in androgen-depleted conditions and facilitates the translocation of AR into nucleus upon activation by growth factors, cytokines and chemokines (4, 7–9). In addition, Src directly phosphorylates, stabilizes and translocates AR to chromatin target sites (9–11). While Src is able to activate AR and serves as its coactivator, Src is reciprocally activated by AR and acts as a downstream effector for AR signaling both in a genomic and nongenomic manner (3, 12). Thus, there is considerable evidence connecting Src signals to prostate carcinogenesis, raising the possibility of targeting Src kinase as a potential therapy. Previous studies demonstrated that Src selective inhibitors such as saracatinib and dasatinib were effective in inhibiting growth, adhesion, migration and invasion of prostate cancer cells *in vitro* (13, 14). In preclinical models, the primary effects of Src inhibitors appear to be the blockade of metastasis (14). We showed that Src inhibitors arrested cell cycle progression but did not induce significant apoptosis, due largely to the concurrent induction of autophagy, which confers a survival advantage (15). The addition of an autophagy inhibitor effectively overcomes the apoptosis-resistance of Src inhibitor treated prostate cancer cells. Presently, several commercial specific oral Src kinase inhibitors are being tested in Phase I and II clinical trials for the treatment of patients with prostate cancer (16, 17). To improve the efficacy of Src inhibitors and its potential use as an adjunctive therapy, it is imperative to understand the Src kinase signals affected by the treatments. Src kinases channel signals through the conventional Ras/Raf/ERK and PI3K/Akt/mTOR pathways (18), but also selectively activate Stat3(19), c-myc (19) and β-catenin (20). These Src induced signals were attenuated in saracatinib-treated PC3 cells (14). In addition to phsophorylation signals, Src activation also leads to the up- and down-modulation of a variety of microRNAs (miRNAs) involved in transformation and oncogenesis (21). Few of these miRNA studies were conducted in prostate cancer cells and the effects of Src inhibitor on the expression of these oncomirs remain unknown.

ERG (Ets-related-gene) is the most frequently overexpressed and translocated oncogene in prostate cancer cells (22, 23) and over 50% of prostate cancer specimens carry a translocation involving the 5′ promoter upstream sequences of the TMPRSS2, an androgen regulated gene, and 3′ coding exons of ERG, resulting in a TMPRSS2-ERG fusion transcripts (24). Most of the ERG coding sequences are retained in the fusion transcript,

which in the context of gene fusion is under the transcriptional control of androgens. TMPRSS2-ERG appears to be a specific biomarker for prostate cancer cells, as normal prostate epithelial cells and benign prostatic hyperplasia (BPH) do not harbor such a translocation. Engineered mice with prostate specific overexpression of ERG develop cellular morphology that resembles precursor-like lesions of human prostate cancer (25–27). When complemented with lesions in the PI3K pathway, progressive prostatic adenocarcinomas were induced in these mouse models (28). Knockdown of ERG diminishes the proliferative, invasive and migratory ability of prostate cancer cells both *in vitro* and *in vivo* (26, 29, 30). Both EZH2 (31), FZD4 (32), ZEB1 (33) and C-MYC (30) are shown to be the downstream targets of ERG that mediate the ERG-induced EMT and block epithelial differentiation. In experimental models TMPRSS2 to ERG translocation can be induced by radiation when combined with activation of AR (31, 34, 35). Under androgen-deprived conditions, in a subset of relapsed tumors, abundant ERG expression, however, could be identified and in castration-resistant VCaP xenograft model harboring TMPRSS2-ERG translocation, ERG expression is maintained under castration conditions (36). The persistent expression of ERG in a subset of castration resistant prostate cancer cases prompted us to investigate other modes of ERG activation that are not solely dependent upon external androgen. In the present study we report the identification of an alternative pathway whereby ERG expression can be upregulated by EGF and SRC via miRNA modulation. Our study has revealed a new crosstalk between the EGF/Src and androgen/AR signaling axes.

RESULTS

Src inhibitors upregulate miR-30 in VCaP cells

To investigate miRNAs regulated by c-Src kinase during the progression of advanced prostate cancer, vertebral metastatic lesion-derived VCaP cells were treated for 24 h with saracatinib (AstraZenca) or PP2 (Pfizer), selective inhibitors of Src-family tyrosine kinases, and the associated changes in miRNA abundance were analyzed by microarrays (containing 132 miRNAs, Signosis). The testing of two different Src inhibitors was intended to minimize the off-target effects of these inhibitors. In the analysis, only miRNAs commonly regulated by both inhibitors were scored. Compared to the control untreated cells, 10 miRNAs were upregulated and 13 miRNAs were downregulated more than 1.5-fold by both inhibitors. Among these miRNAs, the miR-30 family (including miR-30a-5p and miR-30b) was the most increased (Figure 1A). To validate the microarray results, quantitative real-time PCR (qRT-PCR) was performed to analyze the level of mature miR-30 in VCaP and another prostate cancer PC3 cells after 24 h treatments of saracatinib and PP2. Both saracatinib and PP2 significantly increased the expression level of both miR-30a-5p (Figure 1B, left panel) and miR-30b (Figure 1B, right panel) in VCaP and PC3 cells. However, only modest inductions of miR-30c were observed (Supplementary Figure S1). These studies confirmed the microarray data of miR-30 upregulation by Src inhibitors, and showed that such upregulations are not restricted to VCaP cells.

If Src inhibitors upregulate miR-30, Src agonist should suppress miR-30 expression. Signaling by epidermal growth factor (EGF) or its receptor (EGFR) is known to activate Src in prostate cancer cells (9). When VCaP cells were treated with EGF, the expression level of

miR-30a (Figure 1C, left panel) and miR-30b (Figure 1C, right panel) were significantly suppressed by EGF treatment, as expected. By contrast, treatment with gefitinib, an inhibitor of EGFR, upregulated both miR-30a and miR-30b. In addition, the EGF-induced miR-30 downregulation could be completely offset by blocking Src activity with PP2, indicating Src is a major mediator of EGF's modulation of miR-30. We also tested IL-6 and hepatocyte growth factor (HGF), two ligands known to activate Src via their respective receptors (4); both suppressed the expression of miR-30, although their potencies are not as high as EGF (Figure 1C).

miR-30 is downmodulated in prostate cancers

The above results suggest that miR-30 is suppressed by oncogenic signals. Together with the large body of literature showing reduced expression of miR-30 in a variety of tumors (37–39), they support the notion that the miR-30 family may be associated with tumor suppressor functions in prostate cancer. We analyzed the expression pattern of miR-30a and miR-30b in prostate cancer cell lines by qRT-PCR. All prostate cancer cell lines tested expressed a modest but significant level of miR-30, which is lower than the immortalized normal epithelial-derived cell line RWPE-1 (Figure 2A). We then analyzed miR-30 expression in a series of clinical specimens. The mean expression level of miR-30a-5p (Figure 2B, left panel) and miR-30b (Figure 2B, right panel) in tumor samples are significantly lower than that of the benign tissues, consistent with an early report that demonstrated the downmodulation of miR-30 in hormone-refractory prostate cancer (38), as well as prostate CD44+ cancer stem cell population (40).

Ectopic expression of miR-30 inhibits EMT

To test whether miR-30 functionally behaves as a tumor suppressor, we stably overexpressed miR-30b in VCaP and PC3 using lentiviral vector carrying mature miR-30b sequence. Since a major effect of Src-inhibitor is the suppression of tumor invasion and metastasis, we were particularly interested in the effect of miR-30 on genes related to metastasis/EMT. Quantitative RT-PCR was used to measure these genes in pooled populations of VCaP overexpressing miR-30b. Strikingly, the majority of the EMT-associated genes tested were downmodulated by miR-30b overexpression. They include ZEB1, TWIST, ZEB2, SPARC, MMP3 and LIN28, with BMP7, N-cadherin (CDH2), ERG, Notch1 and SNAI1 being the most severely (>80%) affected (Figure 3A). These data suggest that miR-30b inhibits EMT. Further evaluation of the role of miR-30b in EMT modulation was carried out by immunostaining of N-cadherin and E-cadherin (Figure 3B). In this study, we also included cells infected with lentivirus carrying anti-miR30b (antagomir against miR-30b). We found that miR-30b overexpression leads to an increase of E-cadherin and a decrease of N-cadherin expression, and the reverse is true for anti-miR30b. Next, we examined the effect of miR-30 on cell migration and invasion using transwell assay. The cell invasion ability was significantly restrained ($p<0.05$, Figure 3C) in miR-30b-overexpressing VCaP cells. We next overexpressed miR-30b in PC3 cells and showed with wound scratch assay that PC3 cells overexpressing miR-30b migrate much more slowly than the control cells (Figure 3D). Furthermore, to examine whether miR-30 is involved in the suppression of Src-regulated EMT, anti-miR30a/b was overexpressed in VCaP cells followed by treatment with saracatinib in the transwell migration assay. Overexpression of

anti-miR30a/b reversed the inhibition of VCaP migration by saracatinib (Supplementary Figure S2). Taken together, these results suggest that miR-30 functions to maintain the epithelial phenotype and inhibits migration, invasion and EMT of prostate cancer cells.

miR-30 directly targets the ERG 3′UTR

In the EMT genes tested in Figure 3A, ERG was among the most severely suppressed by miR-30. In addition, the expression level of ERG was significantly higher in the human prostate cancer specimens compared to the BPH specimens (Supplementary Figure S3), while the miR-30 expression level was lower in prostate cancer and higher in BPH tissue (Figure 2B). Computational prediction with TargetScan software (http://www.targetscan.org) revealed that an evolutionarily conserved region in the ERG 3′UTR mRNA has a perfect complementary matching region (UGUUUACA) to the seed sequence (ACAAAUGU) of the miR-30 family (Figure 4A). As shown in Figure 4B, 4C and Supplementary Figure S4, TMPRSS2-ERG protein and mRNA expressions were downregulated by miR-30 overexpression in VCaP cells. To examine whether miR-30 attenuates ERG expression through direct targeting of the predicted 3′UTR region, a 42-base pair fragment of the ERG 3′UTR containing the wild-type or mutant miR-30 binding site were constructed downstream of the luciferase gene in a reporter plasmid (UTR-reporter; Figure 4A). 293T cells were transfected with the UTR-reporter plus the negative control miRNA (miR-NC), miR-30a or miR-30b. Only transfection of miR-30a and miR-30b with the wild-type UTR-reporter led to a significant decrease of luciferase activity whereas co-expression of the antagomirs of miR-30 has no effect on the reporter activities (Figure 4D). In addition, the suppressive effects of miR-30a and miR-30b were abolished with the mutant UTR-reporter in which the seed sequences were altered (Figure 4E). Together, these results demonstrate that miR-30 directly targets the ERG 3′UTR, thereby reducing TMPRSS2-ERG expression.

TMPRSS2-ERG expression is regulated by EGF signaling

Our data above showed that inhibiting Src signals augments the expression of miR-30 and that miR-30 negatively regulates ERG expression. Since Src is activated by EGF (via EGFR), we then asked whether inhibiting Src or EGFR would inhibit the expression of TMPRSS2-ERG. We first tested the role of EGF in TMPRSS2-EGR expression and, as shown in Figure 5A, showed that TMPRSS2-ERG was indeed induced dose-dependently by EGF in VCaP cells. VCaP cells were then treated with increasing doses of the EGFR inhibitor AG1478 (AstraZeneca) and Src inhibitors (saracatinib and PP2) and the TMPRSS2-ERG expression was monitored with Western blotting (Figure 5B) and qRT-PCR (Figure 5C). Inhibition of either EGFR signal or Src activity downmodulated TMPRSS2-ERG expression both at the protein and transcript level (Figure 5B and 5C). These data support the hypothesis that TMPRSS2-ERG is regulated by EGF and Src signaling through miR-30 modulation. Thus, we have identified a new way to modulate TMPRSS2-ERG or ERG expression in an androgen independent manner. To our knowledge, this is the first report that showed the modulation of ERG by growth factors and tyrosine kinases.

Ectopic expression of miR-30 and tumorigenesis

TMPRSS2-ERG is known to play a critical role in the malignant transformation of prostate cancer cells. Knockdown of ERG is found to be associated with decreased proliferation, invasion and metastasis of prostate cancer cells *in vitro* and *in vivo* (30, 33). If ERG is an important target of miR-30, we should observe a similar phenotype of miR-30b overexpressor to ERG knockdown cells. To this end, we prepared VCaP cells infected with lentiviral-shRNA targeting ERG to establish a pool of VCaP/shERG cells. There was a significant inhibition of cell growth in response to overexpression of miR-30b or knockdown ERG in VCaP cells compared to the control cells (Figure 6A). To determine if overexpression of miR-30b decreased cell growth *in vivo*, the genetically modified cell lines were subcutaneously injected into NOD/SCID mice. Serial weekly measurements showed tumor growth was suppressed in VCaP/miR-30b implants compared to vector control (Figure 6B).

DISCUSSION

An alternative way of modulating ERG expression

Increasing evidence suggests that overexpression of TMPRSS2-ERG plays a significant role in the transformation, EMT and invasion of prostate cancer. In primary tumors the major driver of the overexpression of TMPRSS2-ERG is androgen. In the present study, we have identified a new signaling pathway, which connects EGF and Src signaling to ERG activation and EMT. This connection is made through the silencing of the miR-30b locus, which targets ERG at its 3′UTR. This alternative mode of modulation at the RNA level should be independent of and complement to the transcriptional regulation mediated by the androgen/AR axis. We also provide data showing EGFR and Src inhibitions are able to modulate TMPRSS2-ERG expression. This is especially relevant in castration-resistant prostate cancer where the AR is aberrantly activated in the absence androgen. By targeting the RNA stability or translation, Src inhibitor offers another way of downmodulating ERG expression.

Src and miRNA modulation

Src mediates oncogenesis by modulating oncogenes as well as oncomirs (41). miR-30 was among the oncomirs downmodulated in Src-transformed cells (21). We report here that miR-30a-5p and miR-30b are the two top upregulated miRNAs by the Src selective inhibitor saracatinib. Similar findings using PP2 substantiated the specificity of the observed response. In a previous study, showed that miR-30b and miR-30c were upregulated by both EGFR and MET in lung cancer cells (42). This discrepancy is most likely due to the cell type specificity and the complex signal network induced by EGF/EGFR.

EZH2 overexpression in advanced prostate cancer leads to epigenetic silencing of developmental regulators and tumor suppressor genes. Regulation of EZH2 that catalyzes trimethylation of histone H3 on Lys27 (H3K27me3) is typically associated with gene repression. Consistent with the observation that Src inhibitor (bosutinib) downmodulates EZH2 (43), we found that Src activation increases the recruitment of EZH2 and H3K27me3 marks on miR-30b locus in VCaP cells (Supplementary Figure S5). The exact mechanism as

to how Src signal activates EZH2, which in turn, suppresses the expression of miR-30 remains to be elucidated. Other common miRNAs upregulated by both Src inhibitors include Let7i, which targets C-MYC. It has long been recognized that Src transcriptionally activates C-MYC. The detailed mechanisms are not fully understood. Let7i suppression by Src signals could be one reason how C-MYC is activated by Src, and miR-30's suppression could be another, since miR-30's target ERG is known to be a direct activator of C-MYC (22, 27, 30).

The role of miRNA-30 in prostate cancer

miR-30 was described as a "hub" for miRNA oncogenesis signal network in solid tumors (37). Its up- or down- modulation has profound impacts on tumorigenesis. In this report, we showed that miR-30 is downmodulated in prostate cancer cells, especially at the metastatic stage. Porkka et al. (38) has identified 15 miRNAs whose expressions are reduced in castration resistant prostate cancer and miR-30a-5p, miR-30b and miR-30c are among them. Liu et al. (40) showed that miR-30a-5p, miR-30c are commonly downmodulated in three CD44+ cancer stem cell lines. Downmodulation of miR-30 is also found in a variety of tumors (38, 39). This is consistent with the tumor suppressor role of miR-30, which has been shown to induce cellular senescence by negatively regulating B-MYB (44), inhibit self renewal and metastasis of breast tumor initiating cells (45), repress the stem cell and cancer phenotypes via targeting LIN28 (46), and suppress EMT and invasive potential of anaplastic thyroid carcinomas (47). Perhaps, noncoincidentally, a significant fraction of predicted miR-30 direct targets are involved in epithelial-mesenchymal transition. We showed potential targets, ERG, SNAI1, SPARC, MMP3, Notch1, LIN28, and ZEB1/ZEB2, are all downmodulated in response to miR-30b overexpression. We have demonstrated that ERG is a direct target of miR-30. Downregulation of ZEB1, TWIST, ZEB2, SPARC, MMP3 and LIN28, BMP7, CDH2, ERG, Notch1 and SNAI1 may either be direct response to miR-30 or secondary to ERG. Prior studies showed SNAIL1 and vimentin are two direct targets of miR-30, which inhibits TGFβ-induced EMT in one case (48) and confers an epithelial phenotype to human pancreatic cells in the other case (49). Consistent with miR-30's role in suppressing EMT, we found VCaP cells overexpressing miR-30b display reduced expression of N-cadherin and lower migratory and invasive ability. Our qRT-PCR results showed that many EMT genes are downmodulated in VCaP. A similar trend is also observed for PC3 cells expressing ETV4, a close homologue of ERG (50) (data not shown). Our data as well as others taken together suggest that miR-30b is a key modulator of EMT, and miR-30's effect is further augmented in VCaP cells by its direct targeting of ERG. In addition to the reversion of EMT, targeting ERG by miR-30b also resulted in the inhibition of VCaP growth both *in vitro* and *in vivo*. Recent study has shown that miR-30b/c target caspase-3, which in turn, regulated TRAIL-induced apoptosis in glioblastoma cells (51). However, in our previous study, neither saracatinib nor PP2 induced any caspase-3 activity or apoptosis in prostate cancer cells (15). Accordingly, no significant apoptosis regulation by miR-30a/b was seen. The results of the present study, and the consistent observation of reduced expression of miR-30 in human prostate cancer specimens, suggest that miR-30 is a bona-fide tumor suppressor in the context of prostate cancer. Restoration of miR-30 function, either by itself or in conjunction with other therapies, may improve the survival by inhibiting the growth and metastasis of castration resistant prostate cancer.

MATERIALS and METHODS

Cell Cultures and Chemicals

All cell lines were obtained from American Type Culture Collection (ATCC). PC-3, LNCaP, CWR22rv1, and Du-145 cells were cultured in RPMI 1640 (Cellgro; Manassas, VA) supplemented with 10% fetal bovine serum (FBS; Cellgro), 1% penicillin and streptomycin (Invitrogen/Life Technologies; Grand Island, NY). 293T and VCaP cells were cultured in Dulbecco's Modified Eagle's medium (DMEM; Cellgro) with 10% FBS, 1 % penicillin and streptomycin. RWPE-1, benign human prostate epithelial cell line (ATCC) was cultured in keratinocyte serum-free media supplemented with bovine pituitary extract and EGF (Invitrogen). All cell lines were maintained in the presence of 5 % CO_2 atmosphere at 37°C. Saracatinib (AZD0530) and Gefitinib were purchased from Selleck Chemicals (Houston, TX). PP2 (AG1879), AG1478, EGF, IL-6, and HGF were purchased from Calbiochem/Upstate/EMD Millipore (Temecula, CA).

Plasmids

The UTR-reporter plasmid was constructed by introducing a 42 base pair miR-30 seed sequence-containing ERG 3′UTR fragment into the 3′ end of firefly luciferase gene in the pCDNA3-Luc vector, which was constructed by cloning the firefly luciferase coding region into the KpnI/BamHI sites of pCDNA3 (Invitrogen). The wild type or mutant ERG 3′UTR-complementary oligonucleotides were purchased from IDT (Integrated DNA Technology; Coralville, IW) and annealed in buffer containing 100 mM potassium acetate, 30 mM HEPES-KOH, pH 7.4, and 2 mM magnesium acetate. To generate short hairpin RNA (shRNA) against ERG, we designed single-stranded primer oligos targeting sequence (5′-GGTGAAAGAATATGGCCTTCCCGAAGGAAGGCCATATTCTTTCACC-3′) by using the BLOCK-iT RNAi Designer (Invitrogen). All the lentiviral miRNA or shRNA expression plasmids were constructed by introducing the annealed oligo duplex into the BLOCK-iT™ Inducible H1 RNAi Entry Vector (Invitrogen).

Microarray and quantitative real-time PCR

Total cellular RNAs were isolated using the Trizol reagent (Invitrogen) according to manufacturer's instructions. Total RNA concentration was quantified by absorbance at 260 nm using spectrophotometer. For miRNA RT-PCR, 5 ng of total RNA was subjected to reverse transcription using the Taqman microRNA reverse transcription kit (Applied Biosystems/Life Technologies; Grand Island, NY) according to the manufacturer's instructions. Each cDNA generated was amplified by quantitative PCR using Universal PCR Master Mix (without AmpErase UNG) with sequence-specific primers from the TaqMan microRNA assays on an Applied Biosystems 7900HT sequence detection system (Applied Biosystems). For the EMT associated gene RT-PCR, 2 μg of total RNA was subjected to reverse transcription using the Superscript III First-Strand Synthesis SuperMix (Invitrogen) according to the manufacturer's instructions. cDNA was quantified by RT-PCR using iQ SYBR Green Supermix (BioRad; Hercules, CA) with the primers listed in Supplementary Table S1 on the BioRad iQ5 Real-Time PCR detection system (BioRad). The expression levels were quantified using comparative *Ct* method (52), and normalized using the

expression of U6 snRNA or glyceraldehyde-3-phosphate dehydrogenase (GAPDH) housekeeping gene.

Luciferase reporter assay

To perform luciferase reporter assay, 293T cells grown in a 24-well plate were contransfected with 200 ng of recombinant pCDNA-Luc, 2 ng of pRL-SV40 renilla luciferase control plasmid (Promega; Madison, WI) and 20 nM miRNA mimics or antagomir using FuGENE 6 transfection reagent (Promega). 48 h after transfection, cells were harvested, and reporter assays were performed using a Dual-Glo Luciferase Assay System (Promega) according to the manufacturer's instructions. Luciferase activity was measured on the GloMax® 96 Microplate Luminometer (Promega).

Western Blotting

Cell pellets were lysed in modified RIPA buffer (20 mM Tris-HCl, pH 7.5, 150 mM NaCl, 1% NP-40, EDTA) containing 1 mM PMSF and 1% complete protease inhibitor cocktail (Roche Applied Science; Indianapolis, IN). After quantification, equal amounts of lysate were separated by SDS-PAGE and then transferred onto PVDF membranes (Millipore; Billerica, MA). Membranes were blocked in 5% nonfat milk and incubated with anti-ERG (1:1000, Santa Cruz Biotechnology; Santa Cruz, CA and Biocare Medical; Concord, CA), anti-β tubulin (1:10000, Sigma; St. Louis, MO), and anti-β actin (1:10000, Sigma) primary antibodies, followed by incubation with goat-anti-rabbit or goat-anti-mouse secondary antibody conjugated with horseradish peroxidase (HRP) (1:5000, Santa Cruz). The protein signals were visualized by fluography using an enhanced chemiluminescence system (Thermo Scientific; Rockford, IL).

Immunofluorescence staining

Cultured Cells (1×10^5) on glasses coverslips were stained by an indirect Immunofluorescence method. Cells were fixed in fixation buffer (4 % paraformaldehyde in PBS, pH 7.4) and permeabilized in PBS buffer containing 0.5% Triton X-100 and 5% BSA. Cells then stained with primary anti-E-cadherin (1:100, Cell Signaling; Danvers, MA) or anti-N-cadherin (1:100, Cell Signaling), followed by incubation with Alexa Fluor® 555-conjugated anti-rabbit or anti-mouse IgG (1:400, Molecular Probe; Eugene, OR) as secondary antibodies. After staining, samples were mounted with SlowFade Gold antifade reagent with DAPI (Molecule Probe) for nuclear counterstain. Images were collected by using microscope with 200X magnification.

Invasion and wound scratch assay

For the invasion assay, cells (2×10^4) were suspended in serum free medium and added into the Matrigel (Becton Dickinson; Franklin Lakes, NJ) coated cell culture inserts of Transwell with 8 μm pore 24 well plate (Corning Life Sciences; Tewksbury MA) for 48 h. Invaded cells on the bottom of the insert membrane were stained with crystal violet then subsequently extracted and detected on a standard microplate reader at 540 nm absorbance. For the wound scratch assay, cells (2×10^5) were seeded in 12-well culture dish and grown up to 90% confluence. A single wound was made in the center of cell monolayer and cell

debris was removed by washing twice with PBS. Complete medium was added and cells were allowed to migrate into the clearing area for 48 h. The wound closure areas were visualized under an inverted microscope with 100X magnification, and the migrated cells were counted.

Proliferation assay

Cells were seeded (2.5×10^4 per well) in triplicates in 48-well plates. Cell growth was monitored by using the cell proliferation kit I (MTT; Roche Applied Science) at day 1, 3, 6, and 9 days according to the manufacturer's instructions.

Xenograft assay

All experimental procedures using animals were approved by the Institutional Animal Care and Use Committee (IACUC) of UC Davis. 1×10^6 cells in 100 μL of 50% Matrigel were subcutaneous injected into the flank of 6 to 8 week old NOD/SCID mice (Jackson Laboratory; Bar Harbor, Maine).

Statistic analysis

Comparisons between experimental conditions and controls were made using GraphPad Prism version 5.01 (GraphPad Software; La Jolla, CA) by two-tailed unpaired Student's *t*-test or two way ANOVA. All results are expressed as mean ± S.D. and p-values <0.05 was considered statistically significant.

Supplementary Material

Refer to Web version on PubMed Central for supplementary material.

Acknowledgments

This work was supported in part by NIH grants (CA150197 and CA165263) and DOD grant (PC093350) to H.J.K. CJK acknowledges the support of DOD postdoctoral fellowship (PC110744). We are grateful to M. Bradnam for excellent editorial assistance of this manuscript.

References

1. Kung HJ. Targeting tyrosine kinases and autophagy in prostate cancer. Horm Cancer. 2011; 2:38–46. [PubMed: 21350583]
2. Tatarov O, Mitchell TJ, Seywright M, Leung HY, Brunton VG, Edwards J. SRC family kinase activity is up-regulated in hormone-refractory prostate cancer. Clin Cancer Res. 2009; 15:3540–3549. [PubMed: 19447874]
3. Cai H, Babic I, Wei X, Huang J, Witte ON. Invasive prostate carcinoma driven by c-Src and androgen receptor synergy. Cancer Res. 2011; 71:862–872. [PubMed: 21135112]
4. Lee LF, Guan J, Qiu Y, Kung HJ. Neuropeptide-induced androgen independence in prostate cancer cells: roles of nonreceptor tyrosine kinases Etk/Bmx, Src, and focal adhesion kinase. Mol Cell Biol. 2001; 21:8385–8397. [PubMed: 11713275]
5. Yang JC, Bai L, Yap S, Gao AC, Kung HJ, Evans CP. Effect of the specific Src family kinase inhibitor saracatinib on osteolytic lesions using the PC-3 bone model. Mol Cancer Ther. 2010; 9:1629–1637. [PubMed: 20484016]
6. Araujo J, Logothetis C. Targeting Src signaling in metastatic bone disease. Int J Cancer. 2009; 124:1–6. [PubMed: 18942061]

7. Desai SJ, Ma AH, Tepper CG, Chen HW, Kung HJ. Inappropriate activation of the androgen receptor by nonsteroids: involvement of the Src kinase pathway and its therapeutic implications. Cancer Res. 2006; 66:10449–10459. [PubMed: 17079466]
8. Lee LF, Louie MC, Desai SJ, Yang J, Chen HW, Evans CP, et al. Interleukin-8 confers androgen-independent growth and migration of LNCaP: differential effects of tyrosine kinases Src and FAK. Oncogene. 2004; 23:2197–2205. [PubMed: 14767470]
9. Guo Z, Dai B, Jiang T, Xu K, Xie Y, Kim O, et al. Regulation of androgen receptor activity by tyrosine phosphorylation. Cancer Cell. 2006; 10:309–319. [PubMed: 17045208]
10. Kraus S, Gioeli D, Vomastek T, Gordon V, Weber MJ. Receptor for activated C kinase 1 (RACK1) and Src regulate the tyrosine phosphorylation and function of the androgen receptor. Cancer Res. 2006; 66:11047–11054. [PubMed: 17108144]
11. Bello D, Webber MM, Kleinman HK, Wartinger DD, Rhim JS. Androgen responsive adult human prostatic epithelial cell lines immortalized by human papillomavirus 18. Carcinogenesis. 1997; 18:1215–1223. [PubMed: 9214605]
12. Zhoul J, Hernandez G, Tu SW, Huang CL, Tseng CP, Hsieh JT. The role of DOC-2/DAB2 in modulating androgen receptor-mediated cell growth via the nongenomic c-Src-mediated pathway in normal prostatic epithelium and cancer. Cancer Res. 2005; 65:9906–9913. [PubMed: 16267015]
13. Nam S, Kim D, Cheng JQ, Zhang S, Lee JH, Buettner R, et al. Action of the Src family kinase inhibitor, dasatinib (BMS-354825), on human prostate cancer cells. Cancer Res. 2005; 65:9185–9189. [PubMed: 16230377]
14. Chang YM, Bai L, Liu S, Yang JC, Kung HJ, Evans CP. Src family kinase oncogenic potential and pathways in prostate cancer as revealed by AZD0530. Oncogene. 2008; 27:6365–6375. [PubMed: 18679417]
15. Wu Z, Chang PC, Yang JC, Chu CY, Wang LY, Chen NT, et al. Autophagy Blockade Sensitizes Prostate Cancer Cells towards Src Family Kinase Inhibitors. Genes Cancer. 2010; 1:40–49. [PubMed: 20811583]
16. Brunton VG, Frame MC. Src and focal adhesion kinase as therapeutic targets in cancer. Curr Opin Pharmacol. 2008; 8:427–432. [PubMed: 18625340]
17. Yu EY, Wilding G, Posadas E, Gross M, Culine S, Massard C, et al. Phase II study of dasatinib in patients with metastatic castration-resistant prostate cancer. Clin Cancer Res. 2009; 15:7421–7428. [PubMed: 19920114]
18. Summy JM, Gallick GE. Treatment for advanced tumors: SRC reclaims center stage. Clin Cancer Res. 2006; 12:1398–1401. [PubMed: 16533761]
19. Bowman T, Broome MA, Sinibaldi D, Wharton W, Pledger WJ, Sedivy JM, et al. Stat3-mediated Myc expression is required for Src transformation and PDGF-induced mitogenesis. Proc Natl Acad Sci U S A. 2001; 98:7319–7324. [PubMed: 11404481]
20. Karni R, Gus Y, Dor Y, Meyuhas O, Levitzki A. Active Src elevates the expression of beta-catenin by enhancement of cap-dependent translation. Mol Cell Biol. 2005; 25:5031–5039. [PubMed: 15923620]
21. Li X, Shen Y, Ichikawa H, Antes T, Goldberg GS. Regulation of miRNA expression by Src and contact normalization: effects on nonanchored cell growth and migration. Oncogene. 2009; 28:4272–4283. [PubMed: 19767772]
22. Petrovics G, Liu A, Shaheduzzaman S, Furusato B, Sun C, Chen Y, et al. Frequent overexpression of ETS-related gene-1 (ERG1) in prostate cancer transcriptome. Oncogene. 2005; 24:3847–3852. [PubMed: 15750627]
23. Tomlins SA, Rhodes DR, Perner S, Dhanasekaran SM, Mehra R, Sun XW, et al. Recurrent fusion of TMPRSS2 and ETS transcription factor genes in prostate cancer. Science. 2005; 310:644–648. [PubMed: 16254181]
24. Wang J, Cai Y, Ren C, Ittmann M. Expression of variant TMPRSS2/ERG fusion messenger RNAs is associated with aggressive prostate cancer. Cancer Res. 2006; 66:8347–8351. [PubMed: 16951141]
25. Klezovitch O, Risk M, Coleman I, Lucas JM, Null M, True LD, et al. A causal role for ERG in neoplastic transformation of prostate epithelium. Proc Natl Acad Sci U S A. 2008; 105:2105–2110. [PubMed: 18245377]

26. Tomlins SA, Laxman B, Varambally S, Cao X, Yu J, Helgeson BE, et al. Role of the TMPRSS2-ERG gene fusion in prostate cancer. Neoplasia. 2008; 10:177–188. [PubMed: 18283340]
27. Zong Y, Xin L, Goldstein AS, Lawson DA, Teitell MA, Witte ON. ETS family transcription factors collaborate with alternative signaling pathways to induce carcinoma from adult murine prostate cells. Proc Natl Acad Sci U S A. 2009; 106:12465–12470. [PubMed: 19592505]
28. King JC, Xu J, Wongvipat J, Hieronymus H, Carver BS, Leung DH, et al. Cooperativity of TMPRSS2-ERG with PI3-kinase pathway activation in prostate oncogenesis. Nat Genet. 2009; 41:524–526. [PubMed: 19396167]
29. Wang J, Cai Y, Yu W, Ren C, Spencer DM, Ittmann M. Pleiotropic biological activities of alternatively spliced TMPRSS2/ERG fusion gene transcripts. Cancer Res. 2008; 68:8516–8524. [PubMed: 18922926]
30. Sun C, Dobi A, Mohamed A, Li H, Thangapazham RL, Furusato B, et al. TMPRSS2-ERG fusion, a common genomic alteration in prostate cancer activates C-MYC and abrogates prostate epithelial differentiation. Oncogene. 2008; 27:5348–5353. [PubMed: 18542058]
31. Yu J, Mani RS, Cao Q, Brenner CJ, Cao X, Wang X, et al. An integrated network of androgen receptor, polycomb, and TMPRSS2-ERG gene fusions in prostate cancer progression. Cancer Cell. 2010; 17:443–454. [PubMed: 20478527]
32. Gupta S, Iljin K, Sara H, Mpindi JP, Mirtti T, Vainio P, et al. FZD4 as a mediator of ERG oncogene-induced WNT signaling and epithelial-to-mesenchymal transition in human prostate cancer cells. Cancer Res. 2010; 70:6735–6745. [PubMed: 20713528]
33. Leshem O, Madar S, Kogan-Sakin I, Kamer I, Goldstein I, Brosh R, et al. TMPRSS2/ERG promotes epithelial to mesenchymal transition through the ZEB1/ZEB2 axis in a prostate cancer model. PLoS One. 2011; 6:e21650. [PubMed: 21747944]
34. Lin C, Yang L, Tanasa B, Hutt K, Ju BG, Ohgi K, et al. Nuclear receptor-induced chromosomal proximity and DNA breaks underlie specific translocations in cancer. Cell. 2009; 139:1069–1083. [PubMed: 19962179]
35. Mani RS, Tomlins SA, Callahan K, Ghosh A, Nyati MK, Varambally S, et al. Induced chromosomal proximity and gene fusions in prostate cancer. Science. 2009; 326:1230. [PubMed: 19933109]
36. Cai C, Wang H, Xu Y, Chen S, Balk SP. Reactivation of androgen receptor-regulated TMPRSS2:ERG gene expression in castration-resistant prostate cancer. Cancer Res. 2009; 69:6027–6032. [PubMed: 19584279]
37. Volinia S, Galasso M, Costinean S, Tagliavini L, Gamberoni G, Drusco A, et al. Reprogramming of miRNA networks in cancer and leukemia. Genome Res. 2010; 20:589–599. [PubMed: 20439436]
38. Porkka KP, Pfeiffer MJ, Waltering KK, Vessella RL, Tammela TL, Visakorpi T. MicroRNA expression profiling in prostate cancer. Cancer Res. 2007; 67:6130–6135. [PubMed: 17616669]
39. Van der Auwera I, Limame R, van Dam P, Vermeulen PB, Dirix LY, Van Laere SJ. Integrated miRNA and mRNA expression profiling of the inflammatory breast cancer subtype. Br J Cancer. 2010; 103:532–541. [PubMed: 20664596]
40. Liu C, Kelnar K, Vlassov AV, Brown D, Wang J, Tang DG. Distinct microRNA Expression Profiles in Prostate Cancer Stem/Progenitor Cells and Tumor-Suppressive Functions of let-7. Cancer Res. 2012; 72:3393–3404. [PubMed: 22719071]
41. Rothschild SI, Tschan MP, Federzoni EA, Jaggi R, Fey MF, Gugger M, et al. MicroRNA-29b is involved in the Src-ID1 signaling pathway and is dysregulated in human lung adenocarcinoma. Oncogene. 2012
42. Garofalo M, Romano G, Di Leva G, Nuovo G, Jeon YJ, Ngankeu A, et al. EGFR and MET receptor tyrosine kinase-altered microRNA expression induces tumorigenesis and gefitinib resistance in lung cancers. Nat Med. 2012; 18:74–82. [PubMed: 22157681]
43. Hebbard L, Cecena G, Golas J, Sawada J, Ellies LG, Charbono A, et al. Control of mammary tumor differentiation by SKI-606 (bosutinib). Oncogene. 2011; 30:301–312. [PubMed: 20818417]
44. Martinez I, Cazalla D, Almstead LL, Steitz JA, DiMaio D. miR-29 and miR-30 regulate B-Myb expression during cellular senescence. Proc Natl Acad Sci U S A. 2011; 108:522–527. [PubMed: 21187425]

45. Yu F, Deng H, Yao H, Liu Q, Su F, Song E. Mir-30 reduction maintains self-renewal and inhibits apoptosis in breast tumor-initiating cells. Oncogene. 2010; 29:4194–4204. [PubMed: 20498642]

46. Zhong X, Li N, Liang S, Huang Q, Coukos G, Zhang L. Identification of microRNAs regulating reprogramming factor LIN28 in embryonic stem cells and cancer cells. J Biol Chem. 2010; 285:41961–41971. [PubMed: 20947512]

47. Braun J, Hoang-Vu C, Dralle H, Huttelmaier S. Downregulation of microRNAs directs the EMT and invasive potential of anaplastic thyroid carcinomas. Oncogene. 2010; 29:4237–4244. [PubMed: 20498632]

48. Zhang J, Zhang H, Liu J, Tu X, Zang Y, Zhu J, et al. miR-30 inhibits TGF-beta1-induced epithelial-to-mesenchymal transition in hepatocyte by targeting Snail1. Biochem Biophys Res Commun. 2012; 417:1100–1105. [PubMed: 22227196]

49. Joglekar MV, Patil D, Joglekar VM, Rao GV, Reddy DN, Mitnala S, et al. The miR-30 family microRNAs confer epithelial phenotype to human pancreatic cells. Islets. 2009; 1:137–147. [PubMed: 21099261]

50. Hollenhorst PC, Paul L, Ferris MW, Graves BJ. The ETS gene ETV4 is required for anchorage-independent growth and a cell proliferation gene expression program in PC3 prostate cells. Genes Cancer. 2011; 1:1044–1052. [PubMed: 21373373]

51. Quintavalle C, Donnarumma E, Iaboni M, Roscigno G, Garofalo M, Romano G, et al. Effect of miR-21 and miR-30b/c on TRAIL-induced apoptosis in glioma cells. Oncogene. 2012

52. Schmittgen TD, Livak KJ. Analyzing real-time PCR data by the comparative C(T) method. Nat Protoc. 2008; 3:1101–1108. [PubMed: 18546601]

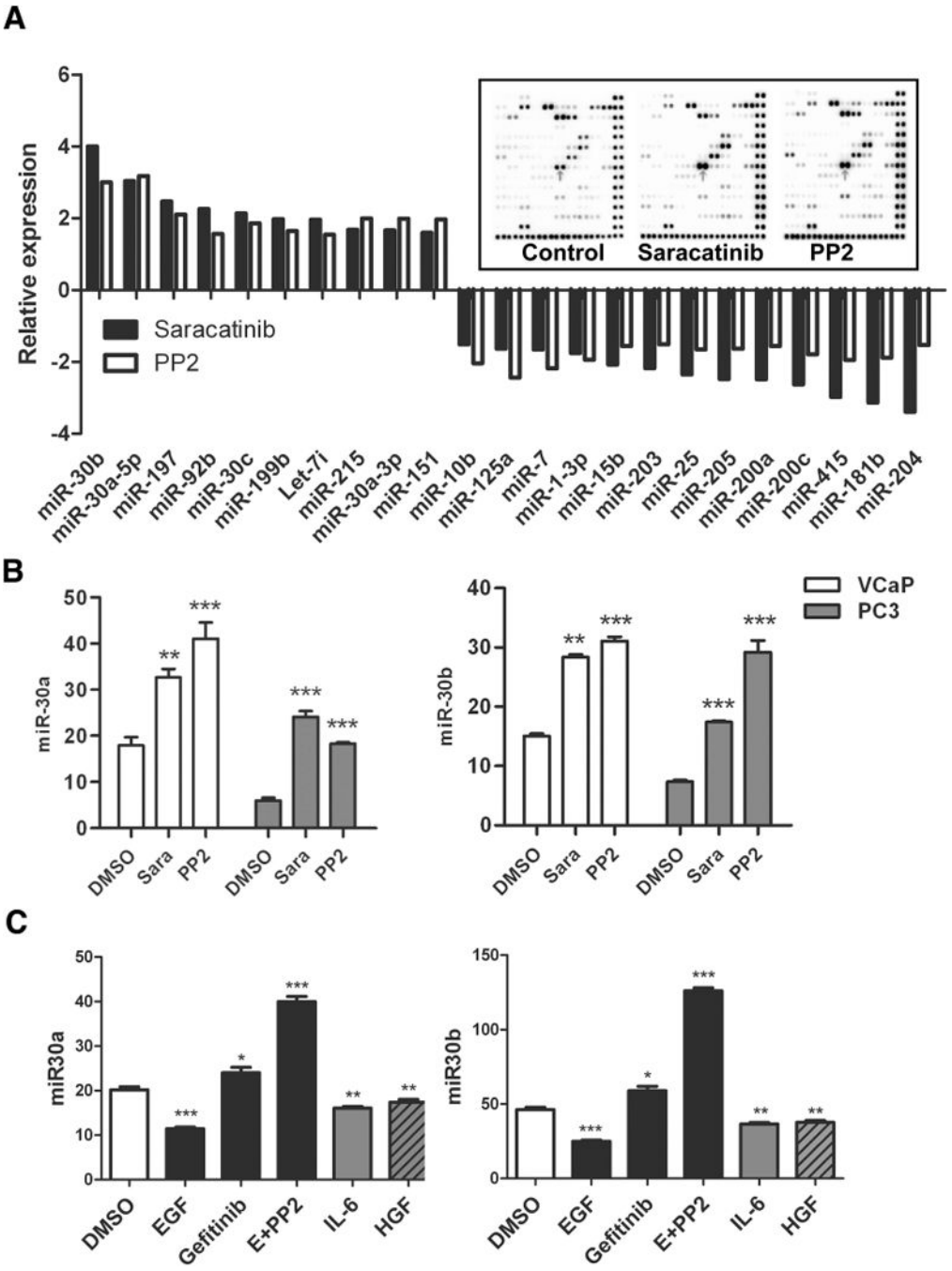

Figure 1.

Src inhibitors upregulate miR-30. (A) Total RNA (5 μg) from VCaP cells treated DMSO, saracatinib (2 μM), or PP2 (10 μM) for 24 h were subjected to Cancer miRNA array assay (Signosis). Each of 132 cancer related miRNA was represented as duplicated spots. Arrow points to miR-30b (insert panel). Compared to the DMSO control, the relative expression level changes greater than 1.5 fold of miRNAs under both treatments are indicated. (B) miR-30a (left panel) and miR-30b (right panel) relative expression levels in response to treatment with DMSO, saracatinib (Sara, 2 μM), or PP2 (10 μM) for 24 h were detected by

qRT-PCR and normalized with U6 snRNA in VCaP and PC3 cells. (C) miR-30a (left) and miR-30b (right) expression levels (as measured by qRT-PCR) following indicated treatments for 24 h in VCaP cells; IL-6 (100 ng/ml), HGF (50 ng/ml), EGF (10 ng/ml), gefitinib (1 μM), and pre-treatment of PP2 (10 μM) for 30 min followed by EGF treatment (E+PP2).*, $p < 0.05$; **, $p < 0.01$; ***, $p < 0.005$.

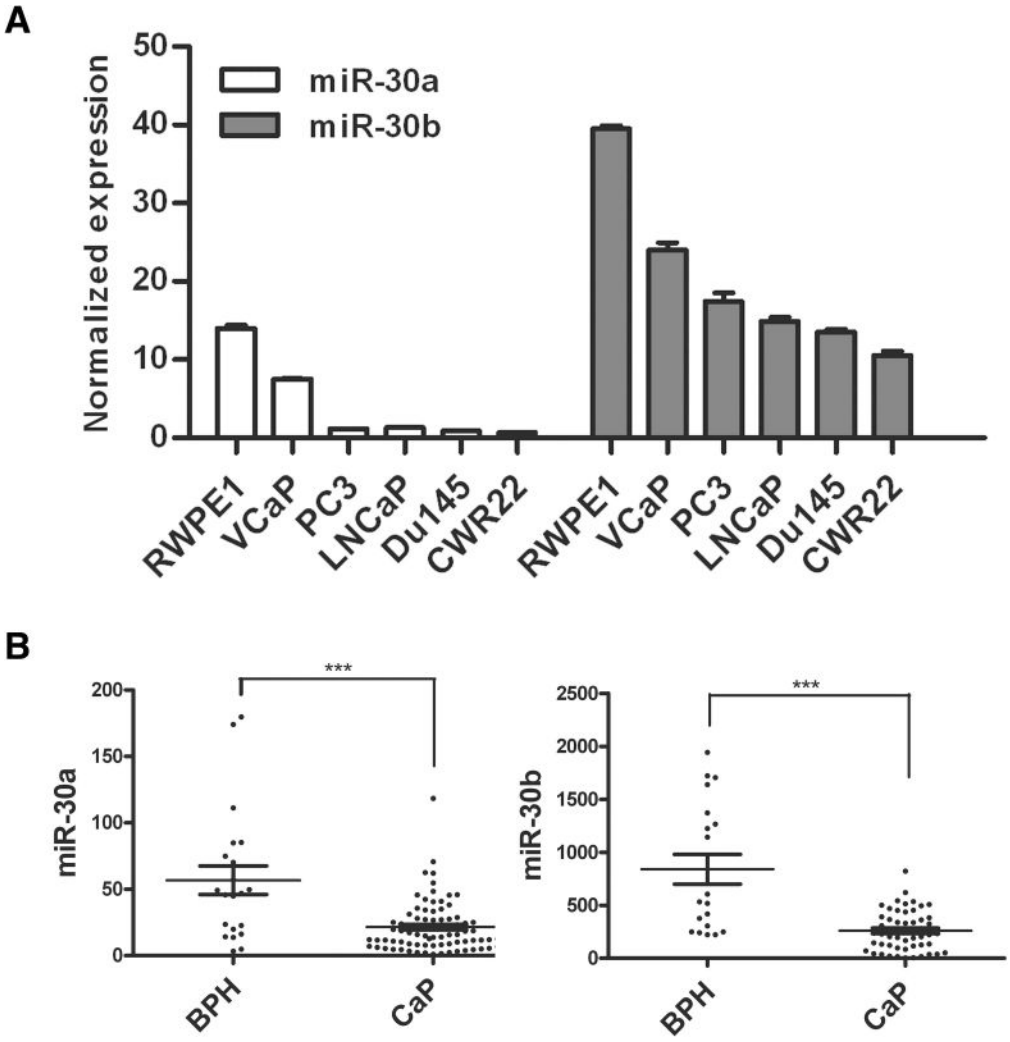

Figure 2.

miR-30 expression is downregulated in prostate cancer. (A) Expression level of mature miR-30a (white) and miR-30b (gray) expression level in indicated prostate cancer and normal cell lines were detected by qRT-PCR and normalized with U6 snRNA. (B) 19 benign prostatic hyperplasia (BPH) and 81 prostate cancer (CaP) specimens (including 11 metastatic pelvic lymph nodes) were obtained fresh from surgical excision. Total RNA was isolated from pulverized frozen tissues. Levels of miR-30a (left panel) and miR-30b (right panel) in each samples was quantitatively analyzed using qRT-PCR and normalized with U6 snRNA. Utilization of human tissue samples was authorized by the UCD Institutional Review Board (UCD IRB#: 200312072-6, approved 2/2/2009).***, $p < 0.005$.

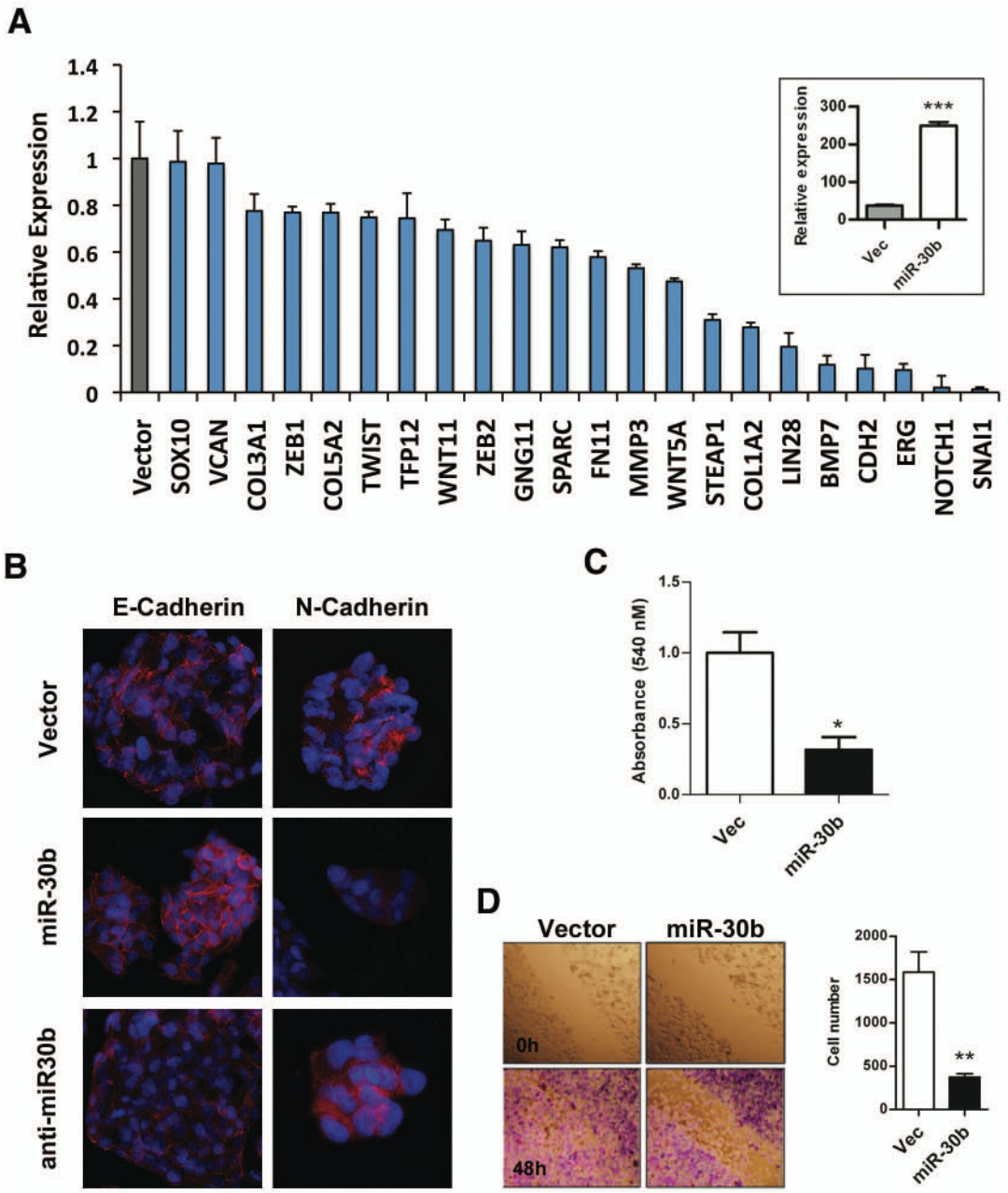

Figure 3.

Ectopic expression of miR-30b inhibits EMT, invasion and motility. (A) Lentiviral infection of empty vector or miR-30b in VCaP cells was selected using zeocin (200 ng/ml). Expression of EMT-associated genes were detected by qRT-PCR and normalized with GAPDH gene expression. Shown are the mean values of the relative expression in miR-30b overexpression versus vector control in VCaP cells. Insert: Expression level of miR-30b in vector (Vec) and miR-30b overexpressing VCaP cells. (B) E-cadherin and N-cadherin immunofluorescence (Magnification 200X). DAPI staining (blue) was used to visualize nuclei. (C) Matrigel invasion of vector and miR-30b overexpressing VCaP cells. Cells (2×10^4) were seeded in transwells for 48 h, and the invading cells were stained with crystal

violet then determined by absorbance at 540 nm. (D) Wound scratch assay. Vector or miR-30b overexpressing PC3 cells (2×10^5) were seeded in 12-well culture dish and grown up to 90% confluence. A single wound was made in the center of cell monolayer. The wound closure areas were visualized under an inverted microscope with 100X magnification (left panel), and the migrated cells were counted (right panel). Scratch assays were performed three times and representative results are shown. *, $p < 0.05$; **, $p < 0.01$; ***, $p < 0.005$.

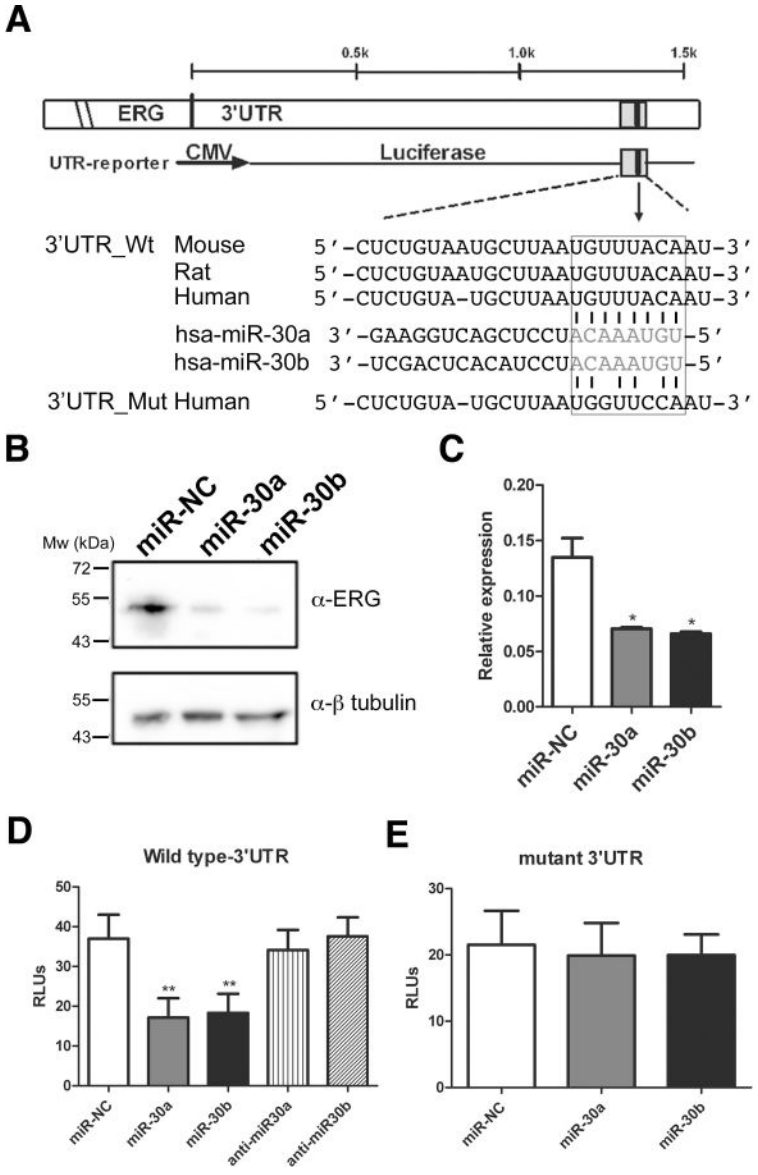

Figure 4.

miR-30 targets ERG. (A) Map of ERG mRNA (human: NM_004449, mouse: NM_133659, rat: NM_133397), together with the landmarks of ERG 3′UTR. The predicted base pairing of the ERG 3′UTR target region and the conserved miR-30 seed sequence (framed) were based on TargetScan software. The sequence of wild type and mutant 3′UTR shows the segment cloned into the luciferase reporter plasmid. (B and C) VCaP cells were transfected with the miR-30a, miR-30b or negative control miRNA (miR-NC) oligos (20 nmol/L) for 48 h. Total cell lysates were analyzed by Western blotting with indicated antibodies (B). Relative mRNA levels of ERG in the transfected cells were analyzed by qRT-PCR assay and normalized with GAPDH gene expression (C). (D and E) 293T cells were co-transfected with wild type (D) or mutant (E) ERG 3′UTR reporter plus indicated miRNA mimics or antagomirs for 48 h. Cell lysates were subjected to dual luciferase assay according to the manufacturer's instructions. *, $p < 0.05$; **, $p < 0.01$.

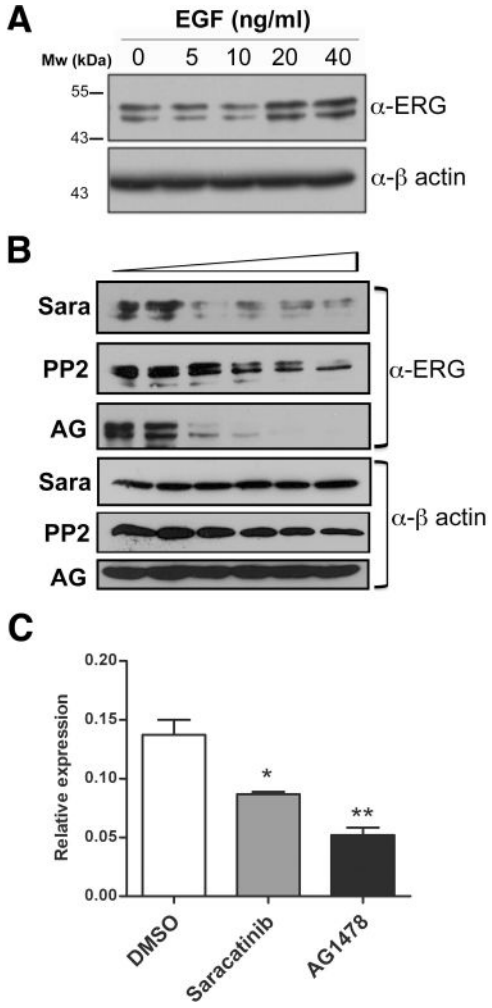

Figure 5.

EGF signaling modulates ERG expression. (A) VCaP cells were treated with indicated doses of EGF for 24h and cell lysates were subjected to Western blotting with anti-ERG and anti-β actin antibodies. (B) VCaP cells were treated with increasing doses of saracatinib (0, 0.5, 1, 2, 4, 8 μM), PP2 (0, 5, 10, 20, 40, 100 μM), and AG1478 (0, 6.25, 12.5, 25, 50, 100 μM) for 24 h and analyzed by Western blotting with indicated antibodies. (C) Corresponding ERG mRNA expression following treatment with saracatinib (2 μM) and AG1478 (25 μM) were detected by qRT-PCR and normalized with GAPDH gene expression. DMSO is used as vehicle control. *, $p < 0.05$; **, $p < 0.01$.

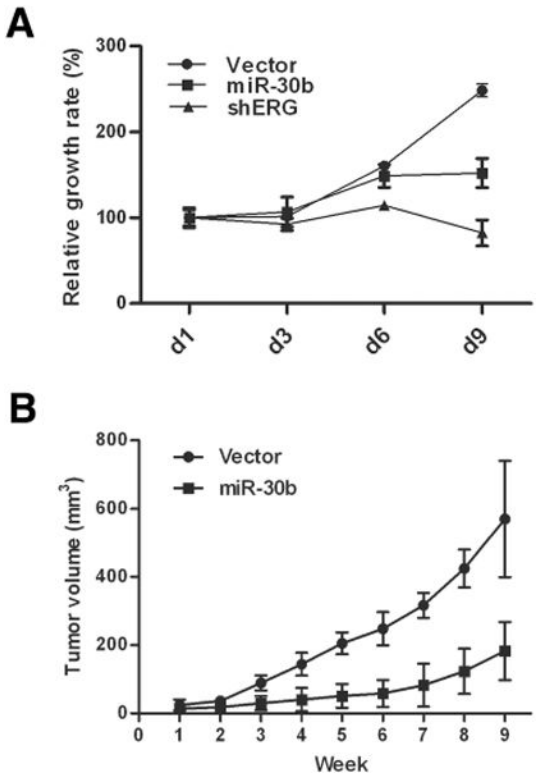

Figure 6.

Ectopic expression of miR-30b inhibits cell growth and tumorigenesis. (A) Proliferation of vector control, miR-30b, and ERG shRNA (shERG) overexpressing VCaP cells were analyzed at day 1, 3, 6, and 9, using the MTT assay as described in Materials and Methods. Cell growth rate is expressed in percentage (%) compared with initial absorbance at day 1. (B) Control or VCaP/miR30b cells (1×10^6) mixed with 50% Matrigel were subcutaneous inoculated into the flanks of NOD/SCID mice (Vector, n=4; miR-30b, n=5). Tumor volumes were monitored weekly by caliper measurements. Results are mean ± standard deviation.